

# Numerical Reproduction and Possible Mechanism of the North-south Difference in Landslide Distribution during the 2018 Hokkaido Eastern Iburi Earthquake

○Dongliang HUANG, Hiroyuki GOTO, Chenlin XIANG

## 1. Introduction

Earthquake-induced landslides often have unique regional distribution characteristics and cause significant damage to the natural environment and severe loss of life and property. This study aims at providing a comprehensive investigation on the critical triggering factor behind the landslide distribution of the 2018 Hokkaido Eastern Iburi Earthquake. It focuses on an interesting phenomenon: although the geological and geomorphological conditions are the same in the north and south sides of the epicenter, the landslide damage is greater in the north side (Fig. 1). This special distribution pattern was reproduced and explained successfully. The contribution of the special phase components to the slope failure is confirmed. The proposed method can be applied to the risk analysis in the regional landslide hazard against future earthquakes.

## 2. Methodology

The representative slope model composed of slope height ( $H$ ) and slope angle ( $\theta$ ) was first obtained through the statistical analysis of the relationship between landslides (Kita, 2014) and slopes (Fig 2). Then, the seismic waveforms in the hillside were synthesized by combining the ground motion model

(Morikawa and Fujiwara, 2013) and the phase characteristics extracted from the 4 downhole records (KiK-net, [www.kyoshin.bosai.go.jp](http://www.kyoshin.bosai.go.jp)) in the vicinity (Fig. 3). Source model is from Asano and Iwata (2019).

The 100 points in the hillside was considered. The synthetic waveforms at each site were generated using a proposed distance weighted spatial interpolation method and a spectrum matching technique (Alexander et al., 2014). After finite difference simulation of slope failure, landslide susceptibility maps were generated in terms of the residual displacement (separate EW/NS).

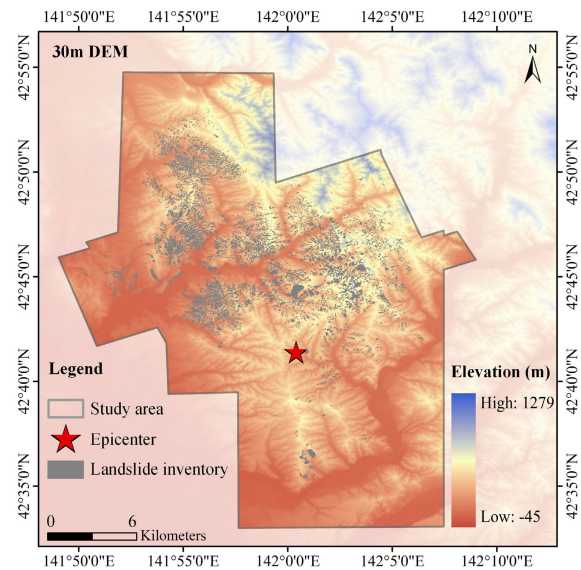


Fig. 1 Geomorphological conditions of study area.

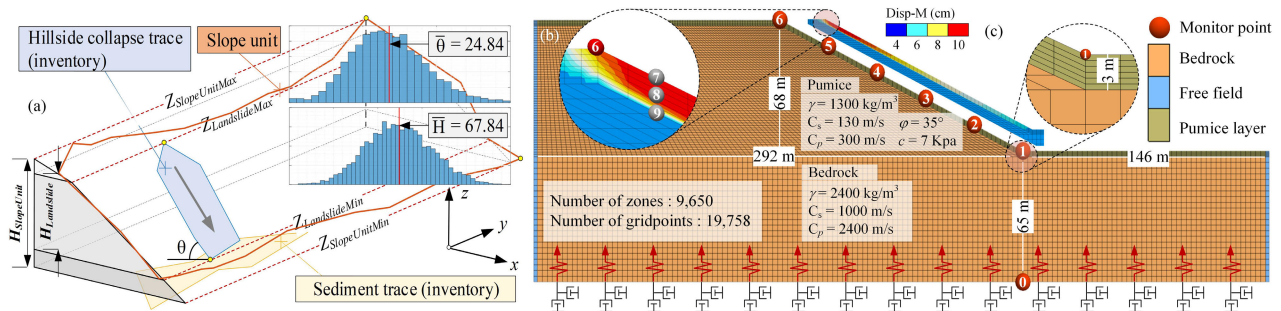


Fig. 2 Relationship between landslides and slopes (a); the representative model (b) and its failure pattern (c).

### 3. Results

Similar to reality, the simulated failure pattern of slope is characterized as a shallow landslide in the loose and crushable surficial pumice material (Fig. 2c). Combined the results of the EW (Fig. 4) and NS (Fig. 5) groups in residual displacement, the sites with larger values are located almost to the north side of the epicenter and cover the landslide area described in the inventory. Therefore, the spatial pattern in which landslide damage is greater in the north side of the epicenter was reproduced successfully. In addition to the traditional understanding of PGA and PGV, the specific phase components of the synthetic waveforms are found to be critical in the evolution of landslides.

### Acknowledgments

Financial supports for this study were partially provided by the Chinese Scholarship Council (CSC, Nos. 202106370143, 202107000093). The content in this abstract have been already submitted to journal Engineering Geology (ENGEO-D-23-00018) and under review now. More details can be found in the journal paper version.

### References

- Alexander, N.A., Chanerley, A.A., Crewe, A.J., Bhattacharya, S., 2014. Obtaining spectrum matching time series using a reweighted volterra series algorithm (RVSA). *Bull. Seismol. Soc. Am.* 104, 1663–1673.
- Asano, K., Iwata, T., 2019. Source rupture process of the 2018 Hokkaido Eastern Iburu earthquake deduced from strong-motion data considering seismic wave propagation in three-dimensional velocity structure. *Earth, Planets Sp.* 71, 101.
- Kita, K., 2018. Map of slope failure traces in the 2018 Hokkaido Eastern Iburu Earthquake created using orthographic projection images [WWW Document].
- Morikawa, N., Fujiwara, H., 2013. A New Ground Motion Prediction Equation for Japan Applicable up to M9 Mega-Earthquake. *J. Disaster Res.* 8, 878–888.

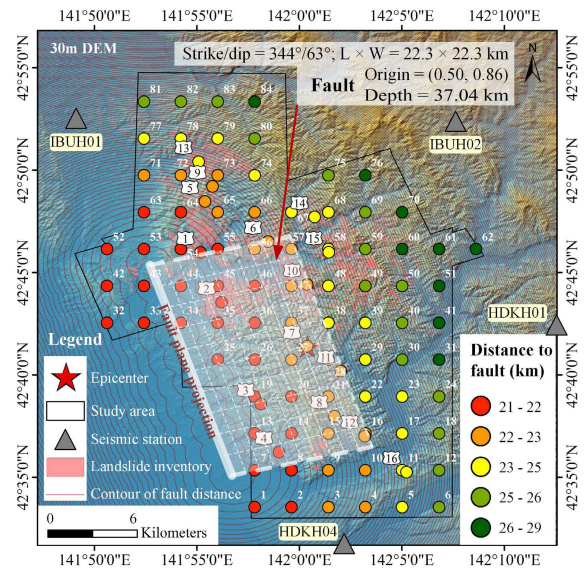


Fig. 3 Interpolation points and their distances to fault.

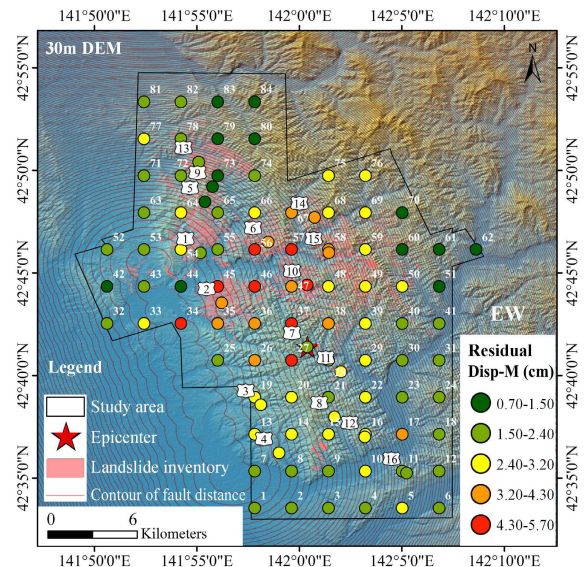


Fig. 4 Pattern of residual displacement (EW group).

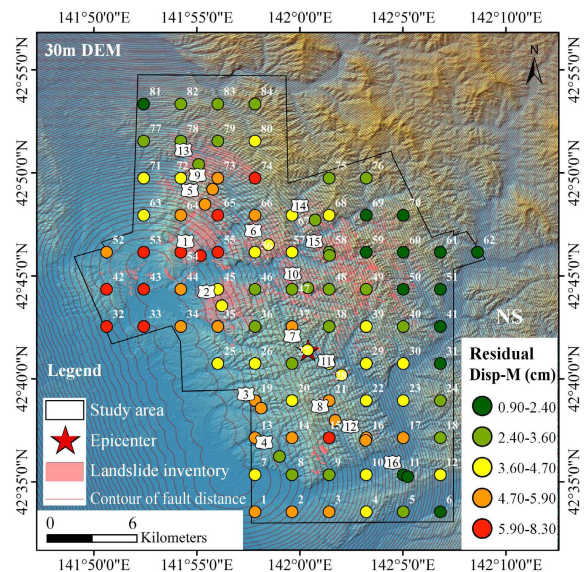


Fig. 5 Pattern of residual displacement (NS group).